sLHC Project Note 0025

2010-11-12

margarita.garcia.tudela@cern.ch

Updated end-to-end simulations of Linac4

M. Garcia Tudela, G. Bellodi, M. Eshraqi, L.M Hein, J.B Lallement, A. Lombardi, P.A Posocco, E. Sargsyan.

Summary

After a first definition stage, some changes were applied to Linac4 layout in order to refine some design choices and to improve the performances of the line. Therefore a new campaign of simulations was carried out, to detect mismatched points, and the obtained results are presented in this note.

1. Introduction

The overall Linac4 layout was determined based on general consideration of beam dynamics and RF. A campaign of end to end simulations was performed with the purpose of identifying bottlenecks, and acceptance limitations. See ref [1].

After this first definition stage, some changes have been applied to this layout in order to refine some design choices and to improve the performance of the line. Thus, a new campaign of simulations was carried out.

Figure 1.1 shows a schematic of Linac4. The present layout consists of a RF volume source (similar to the one in DESY), which provides an H- beam at 45 keV. The matching of the beam to the RFQ is done in the Low Energy Beam Transport line with two magnetic solenoids. The first RF acceleration stage, from 45 keV to 3 MeV, is performed by a 3 meters, 4 vanes Radio Frequency Quadrupole resonating at 352.2 MHZ [2]. After the RFQ, the pulse time structure of the beam is modified (in order to avoid losses during the injection into the PS Booster) in the MEBT by a beam chopper consisting of 4 deflecting plates. The MEBT provide also the beam matching to the following structures. Then, three types of accelerating structures bring the energy up to 160 MeV: a Drift Tube Linac (DTL) up to 50 MeV, a Cell-Coupled Drift Tube Linac (CCDTL) up to 102 MeV and finally, a Pi-Mode Structure (PIMS) to the final energy.

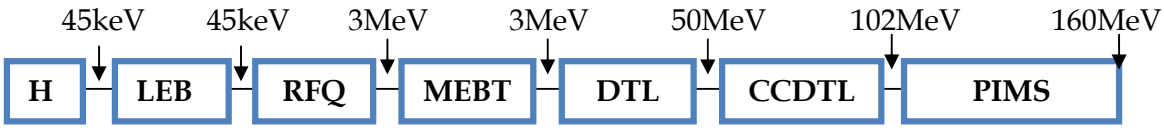

Figure 1.1 Linac4 Layout.

The beam dynamics in each structure were studied and analyzed independently. In addition end-to-end simulations starting from the source were performed with the multiparticle simulation codes PathManager [3] and TraceWin [4]. Both codes give similar results, and the maximum deviation between them is 5% in the worst case [1]. Therefore only PathManager results are presented in this note.

sLHC-Project-Note-0025 12/11/2010

This is an internal CERN publication and does not necessarily reflect the views of the CERN management.

2. Beam dynamics in the LEBT

The low energy beam transport line (LEBT) matches the beam from the source to the RFQ. It consists of 2 solenoids providing the transverse focusing to obtain the matched twiss parameters at the entrance of the RFQ. The schematic layout is represented in figure 2.1. The length of the LEBT is 1.82 meters.

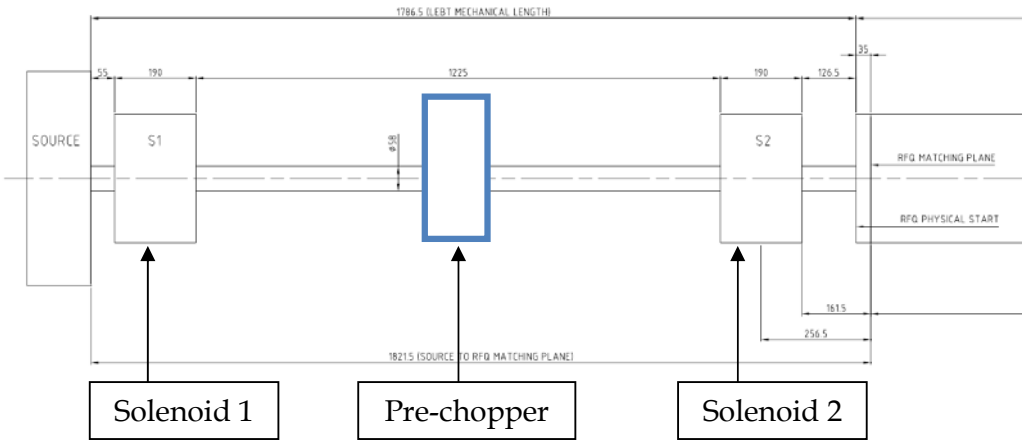

Figure 2.1 LEBT Scheme.

A pre-chopper device is included in the LEBT in order to deflect the head tail of the beam corresponding to the stabilization time of the RF Source. This device could be used in combination with the chopper in the MEBT to reduce the beam pulse length, although other approaches were studied to have the possibility of varying the beam current, in the 3MeV part of Linac4 [5].

Due to the high current and the low energy, space charge compensation is needed in the LEBT. The space charge effects can be compensated by the capture of positive ions by the beam; this is made possible injecting a gas into the vacuum chamber.[6]

For the beam dynamics simulations, it is assumed:

- A uniform input beam distribution with transverse emittance in both planes (x, y) of 0.25 π.mm.mrad
- A constant beam current of 80 mA from the source and 70 mA at the entrance of the RFQ. These 10 mA are taken as margin of unexpected losses due to the space charge compensation effects.
- The extraction energy of the source is 45 keV.
- Energy spread (+/- 0.5 keV)

The Twiss parameters of the LEBT input beam are reported in the following table.

	α	B	ε_{rms}	$\varepsilon_{90\%}$
x	-6.64	0.36 mm/ π mrad	0.25 π mm mrad	0.90 π mm mrad
y	-6.64	0.36 mm/ π mrad	0.25 π mm mrad	0.90 π mm mrad

Table I. Source output beam parameters

Figure 2.2 show the RMS beam size along the LEBT.

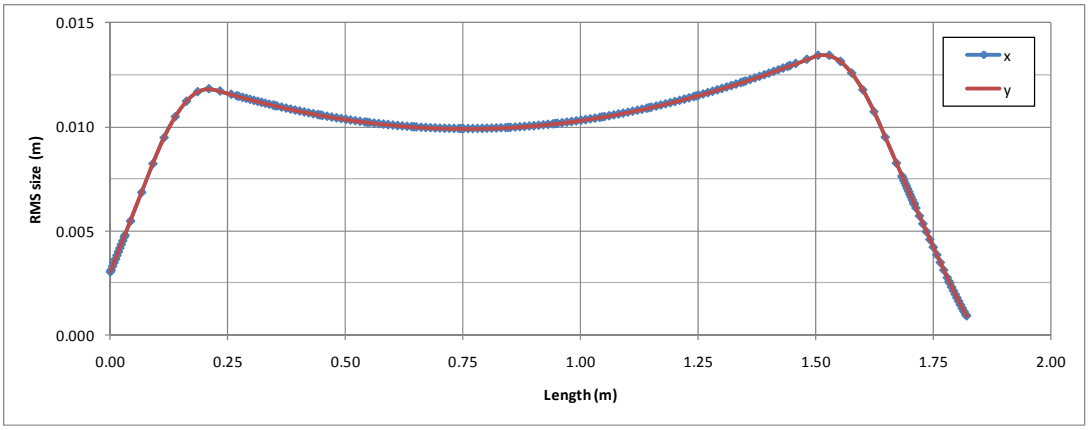

Figure 2.2 RMS beam size along the LEBT.

The twiss parameters and the emittances at the output of the LEBT are summarized in the table below.

	α	B	ε_{rms}	$\varepsilon_{90\%}$
x	1.17	0.03 mm/ π mrad	0.27 π mm mrad	1.06 π mm mrad
y	1.16	0.03 mm/ π mrad	0.27 π mm mrad	1.06 π mm mrad

Table II. LEBT output beam parameters

The RMS and 90% emittance growth are reported in Table III.

	ε_{rms}	$\varepsilon_{90\%}$
x	8.16 %	18.56 %
y	8.37 %	18.86 %

Table III. RMS and 90% emittance growth in the LEBT.

3. Beam dynamics in the RFQ

A Radio Frequency Quadrupole accelerator (RFQ) is required to bunch the H- beam from the ion source at 45 keV and accelerate it up to the energy of 3 MeV.

When the Linac4/SPL project started, the first option for providing a 3 MeV injector to the accelerator was represented by the IPHI RFQ, a powerful accelerating structure, 6-m long, designed to operate in CW mode [7]. Simple considerations about the Linac4 duty cycle, going from 0.08 % to 6 %, suggest that a dedicated RFQ would make the injector considerably gain in efficiency, by reducing its total length to 3 m, and it would produce a relevant simplification of the RF system to feed the RF power required by the accelerator [2]. The characteristics of Linac4 RFQ are summarized in Table IV.

Linac4 RFQ Parameter	***Value***	***Units***
Frequency	352.2	MHz
Length	3.06	m
Vane voltage	80.62	kV
Minimum aperture a	0.18	cm
Maximum modulation	2.36	
Average aperture r0	0.33	cm
ρ/r0	0.85	
Minimum longitudinal radius	0.9	cm
Max field on pole tip	34	MV/m
Kilpatrick value	1.84	
Focusing parameter	5.7	
Acceptance at zero current	1.7	π mm mrad
Final synchronous phase	-22	deg

Table IV. Main parameters of the Linac4 RFQ Design.

The nominal optics is calculated with the matched beam from the LEBT. The simulation was performed with PARMTEQM[8]. Figure 3.1 shows the transverse and longitudinal beam envelopes.

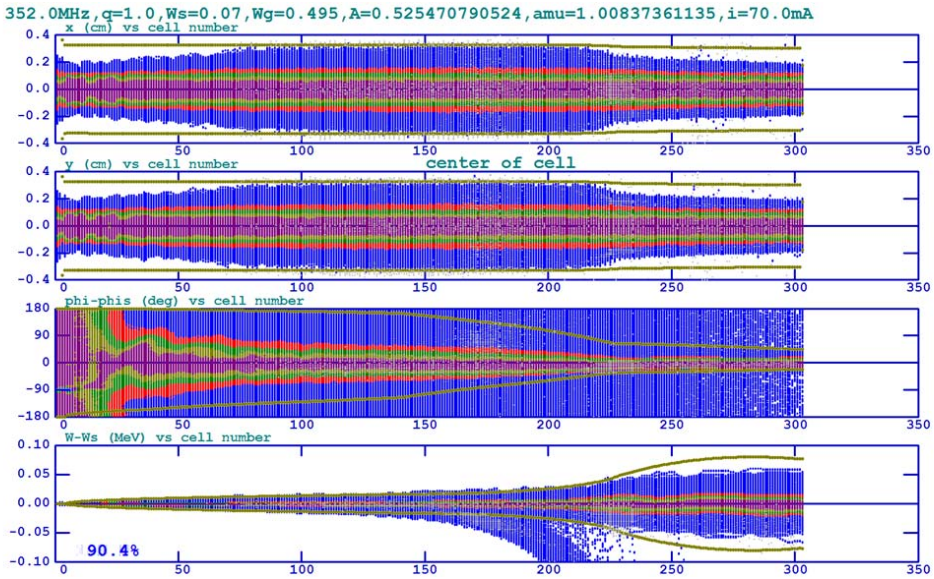

Figure 3.1 Beam dynamics in the RFQ.

Figure 3.2 presents the RFQ output beam shape, in the three phase spaces and in x-y.

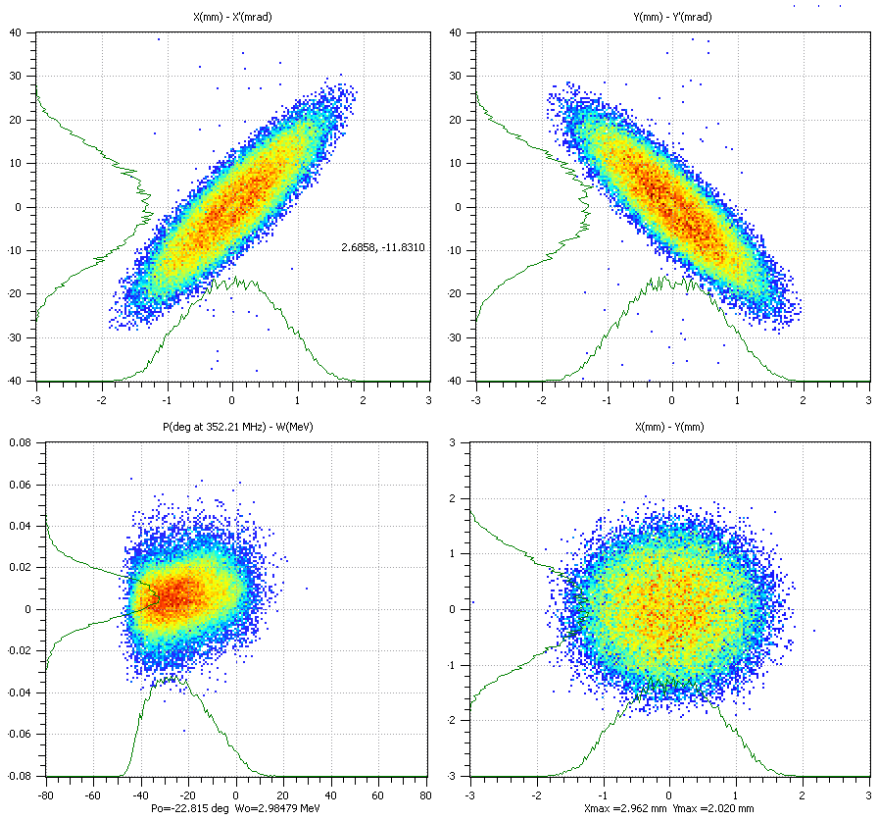

Figure 3.2 Beam phase spaces at the output of the RFQ. PlotWin [4].

The twiss parameters and the emittances at the output of the RFQ are summarized in the table below. The RMS and 90% emittance growth are reported in Table VI.

	α	β	ε_{rms}	$\varepsilon_{90\%}$
x	1.85	0.14 mm/ π mrad	0.24 π mm mrad	1.03 π mm mrad
y	-1.88	0.14 mm/ π mrad	0.24 π mm mrad	1.02 π mm mrad
z	-0.22	1122.38 deg/ π MeV	0.13 π deg MeV	0.54 π deg MeV

Table V. RFQ output beam parameters

	ε_{rms}	$\varepsilon_{90\%}$
x	- 9.96 %	-3.33 %
y	- 10.30 %	-2.79 %
z	-	-

Table VI. RMS and 90% emittance growth in the RFQ.

4. Beam dynamics in the Chopper Line

For the end-to-end simulation the output distribution of the RFQ with 92841 macro-particles was considered.

The H- current from the source, 80 mA, is reduced to 65 mA after the RFQ (we consider 10mA margin of losses in the LEBT) and to 40 mA average in the pulse after chopping. The micro-bunch current of 65 mA is such, that space-charge effects are dominating at low energy and therefore some beam degradation can be appreciated along the line.

The chopper line (also called MEBT) is used to modify the time structure of the pulse avoiding losses during the injection into the PS Booster. It removes the bunches that would fall outside the RF bucket of the PSB (133 out of 355), and creates the gaps corresponding to the rising time of the kicker magnets in the transfer line beam injection region. This part of the layout consists of 3 buncher cavities, 11 quadrupoles (two of them housing two chopper plates separated by 20mm) and a dump which collects the chopped bunches and acts as a rudimentary collimator. The MEBT length is 3.90 m. See Figure 4.1.

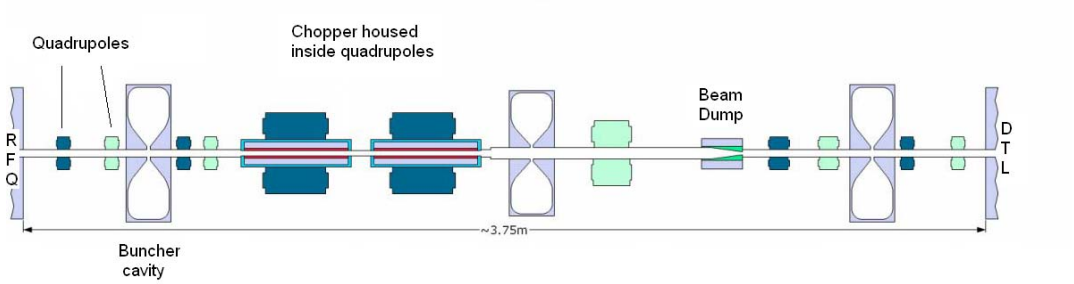

Figure 4.1 MEBT Scheme.

The optic in the chopper was recently reviewed to allow better beam dynamics performance, and higher chopping efficiency. Twiss parameters of the input beam (output of the RFQ) are summarized in table V.

Figures 4.2 and 4.3 show the RMS beam size and the RMS normalized emittances along the structure, with chopper OFF. For the beam dynamics in Linac4 with chopper ON see section 10.

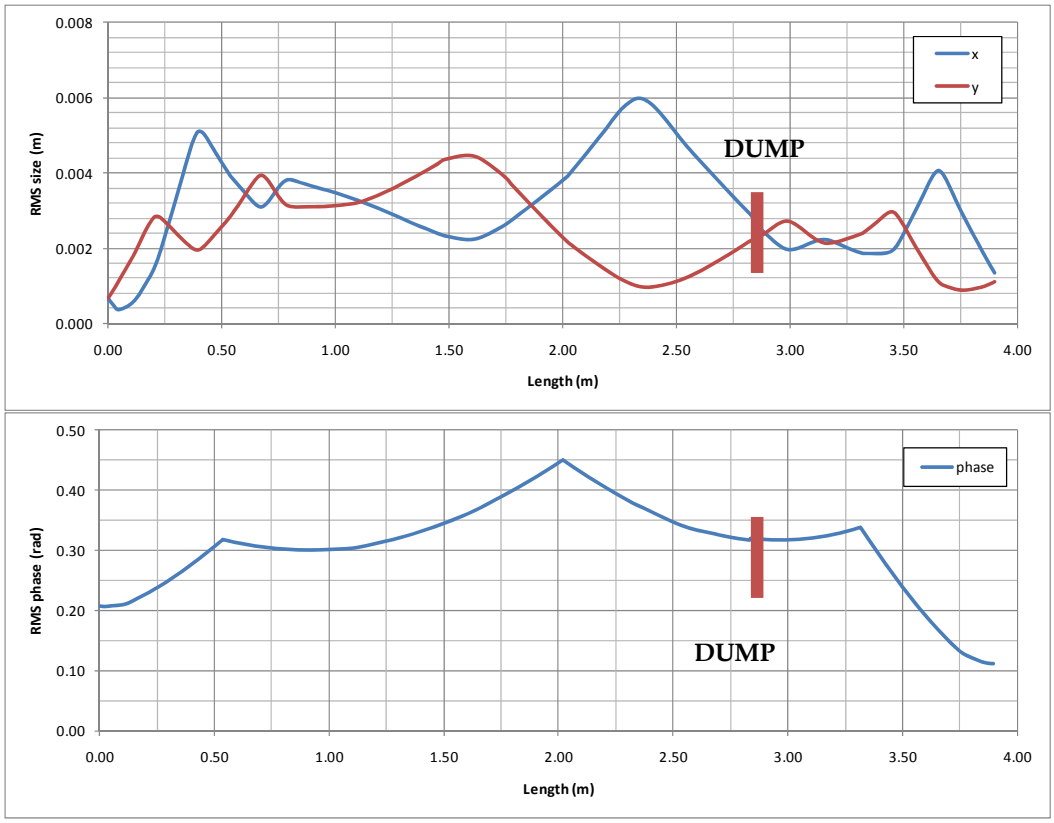

Figure 4.2 RMS beam size along the Chopper Line.

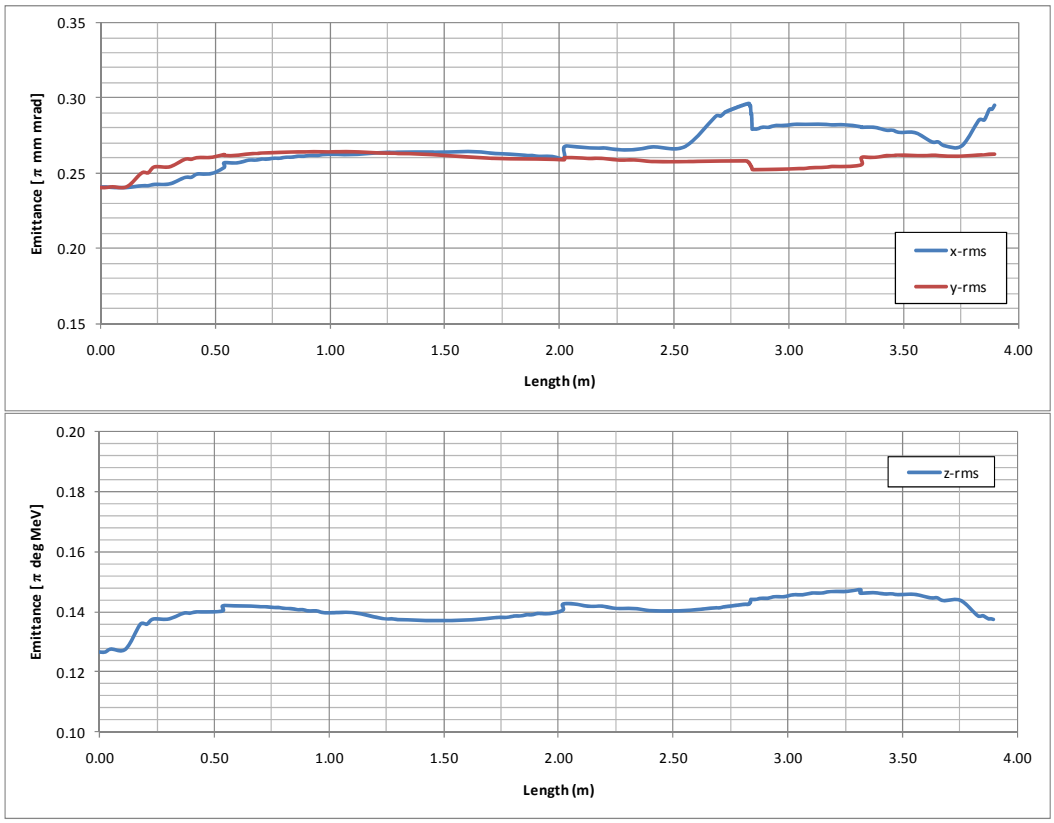

Figure 4.3 RMS normalized emittance along the Chopper Line.

Some emittance increase in x plane is detected at the end of the chopper line due to space charge effects and the strong focusing required to match the beam to the DTL.

The transmission along the MEBT is 96.31%. Main part of the particles is lost in the dump. The MEBT output peak current is 62.6 mA.

The twiss parameters and the emittances at the end of the MEBT are summarized in the table below. The RMS and 90% emittance growth are reported in Table VIII.

	α	β	ε_{rms}	$\varepsilon_{90\%}$
x	3.68	0.48 mm/ π mrad	0.29 π mm mrad	1.25 π mm mrad
y	-1.06	0.36 mm/ π mrad	0.26 π mm mrad	1.11 π mm mrad
z	-0.012	299.76 deg/ π MeV	0.14 π deg MeV	0.58 π deg MeV

Table VI. Chopper Line output beam parameters.

	ε_{rms}	$\varepsilon_{90\%}$
x	22.50 %	21.59 %
y	8.91 %	8.54 %
z	8.61 %	11.8 %

Table VIII. RMS and 90% emittance growth in the Chopper Line.

Figure 4.4 shows the Chopper Line output beam shape, in the three phase spaces and in x-y.

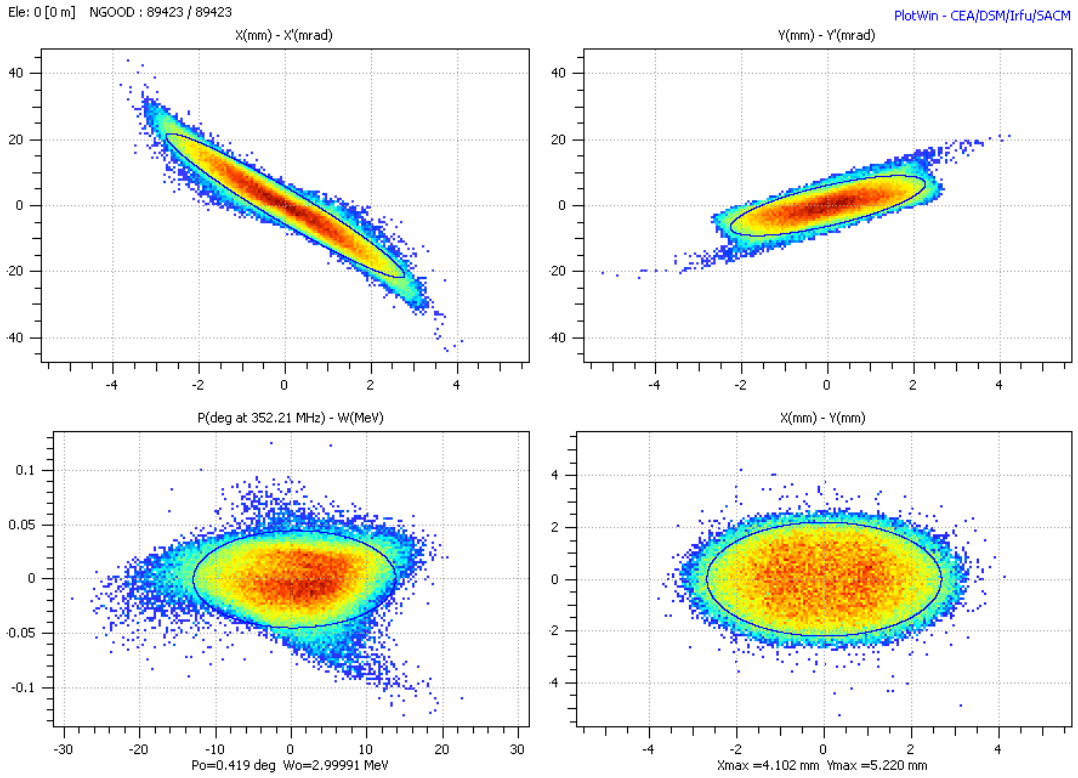

Figure 4.4 Beam phase space at the output of the Chopper Line.

5. Beam dynamics in the DTL

The drift tube linac, DTL, is made of 3 tanks and it accelerates the beam from 3 MeV to 50 MeV. It comprises a total of 114 laser-welded drift tubes containing a PMQ each.The total DTL length is 19.08 m.

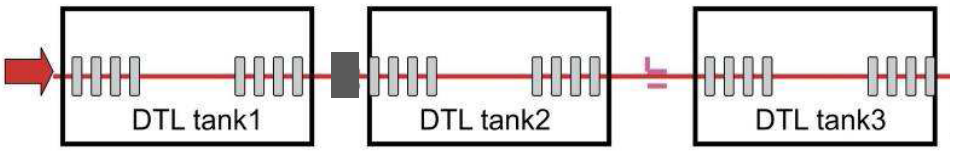

Figure 5.1 Scheme of the DTL.

The focusing scheme in this structure was reviewed during the last months and it was set to FFDD along the 3 tanks in order reduce the beam loss in the presence of gradient and alignment errors [9].

Table IX depicts in more detail each tank.

DTL TANK	Number of cells	Length (m)	Output Energy (MeV)
1	*39*	*3.90*	*11.87*
2	*42*	*7.35*	*31.56*
3	*30*	*7.25*	*50.28*

Table IX. DTL Tanks depiction.

As in the previous sections, simulations results obtained with PathManager are reported below, using the Chopper Line output as DTL input beam, see table VI for twiss parameters. This beam has 89423 macro-particles and the input beam current is 62.6 mA.

Figures 5.2 and 5.3 show the RMS beam size and the RMS normalized emittances along the structure.

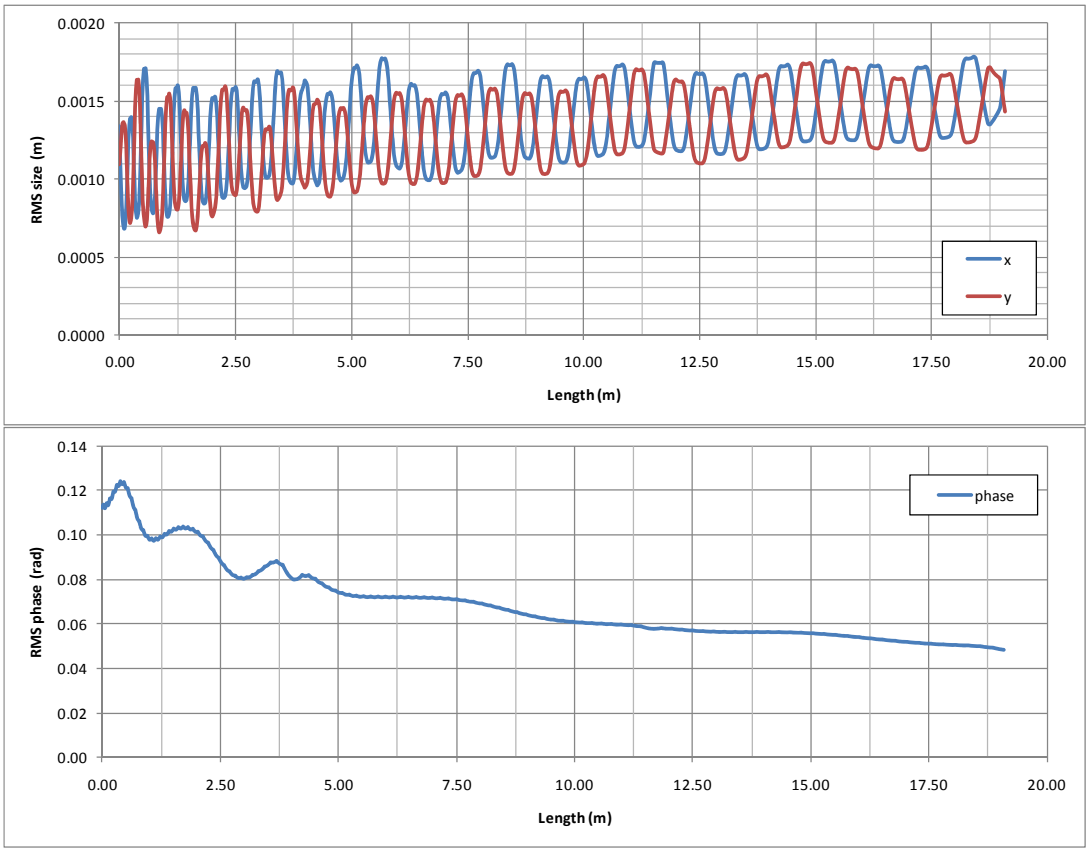

Figure 5.2 RMS beam size along the DTL.

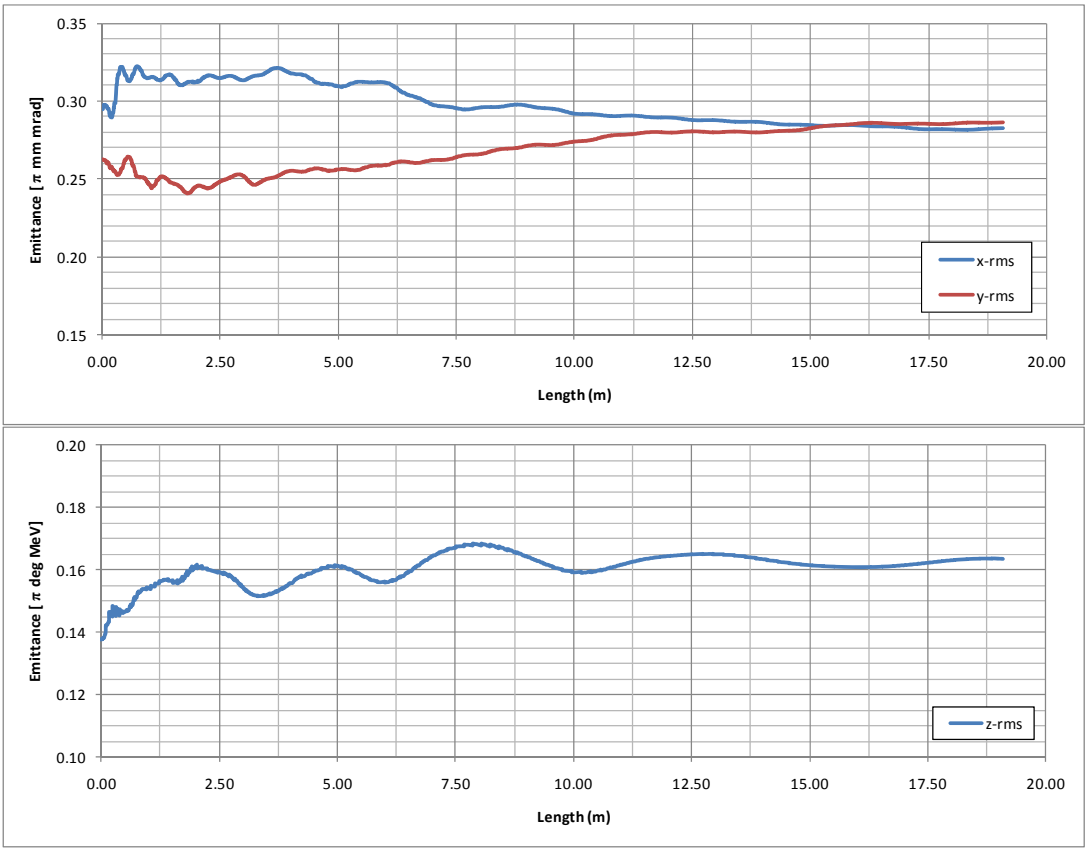

Figure 5.3 RMS normalized emittance along the DTL.

Transverse emittance exchange occurs along the DTL leading to level off the x and y emittances at the end of the structure. The transmission of the DTL is 100%, and the output energy is 50.28 MeV.

The twiss parameters and the emittances at the end of DTL are summarized in the table below. The RMS and 90% emittance growth are reported in Table XI.

	α	β	ε_{rms}	$\varepsilon_{90\%}$
x	-4.73	3.35 mm/ π mrad	0.28 π mm mrad	1.17 π mm mrad
y	3.42	2.37 mm/ π mrad	0.29 π mm mrad	1.19 π mm mrad
z	-0.21	47.13 deg/ π MeV	0.16 π deg MeV	0.68 π deg MeV

Table X. DTL output beam parameters.

	ε_{rms}	$\varepsilon_{90\%}$
x	-4.14 %	-6.07 %
y	9.08 %	6.18 %
z	18.99 %	16.04 %

Table XI. RMS and 90% emittance growth in the DTL.

Figure 5.4 shows the DTL output beam shape, in the three phase spaces and in x-y.

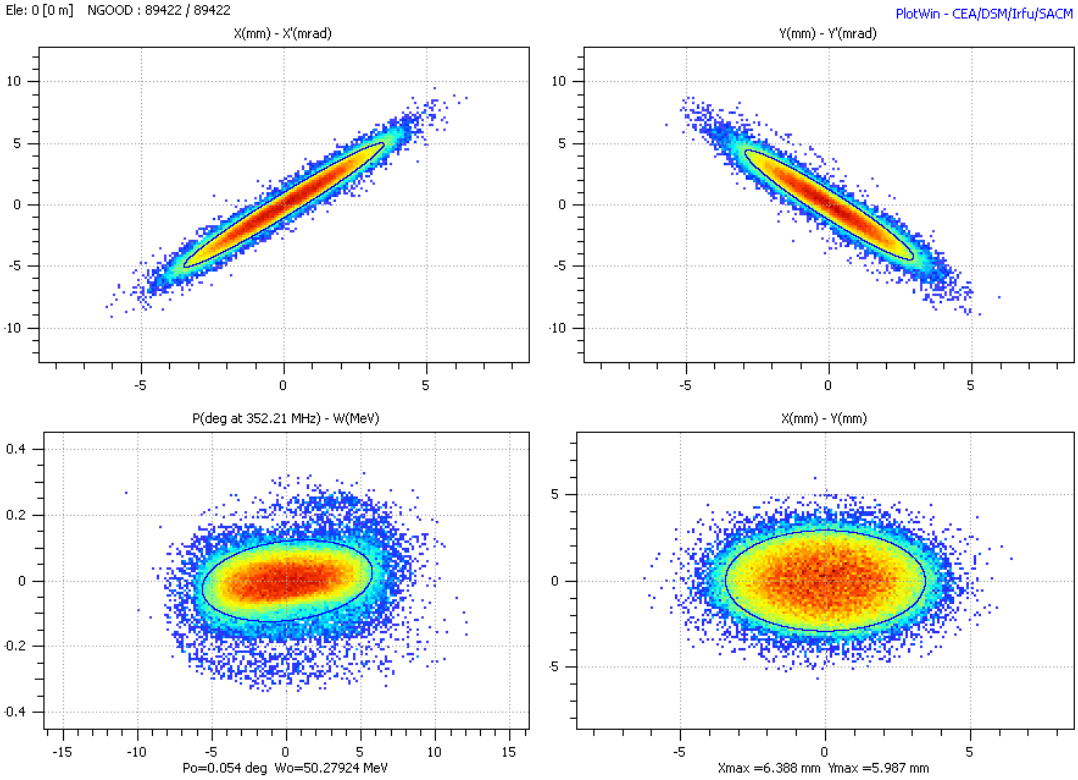

Figure 5.4 Beam phase space at the output of the DTL. PlotWin.

6. Beam dynamics in the CCDTL

The acceleration from 50 MeV to 102 MeV is provided by a Cell Coupled Drift Tube LINAC (CCDTL) working at 352.2 MHz. The CCDTL is made of 7 modules; every module comprises 3 tanks with two drift tubes each, and connected by coupling cells. See figure 6.1.The total length of this structure is 24.9 meters.

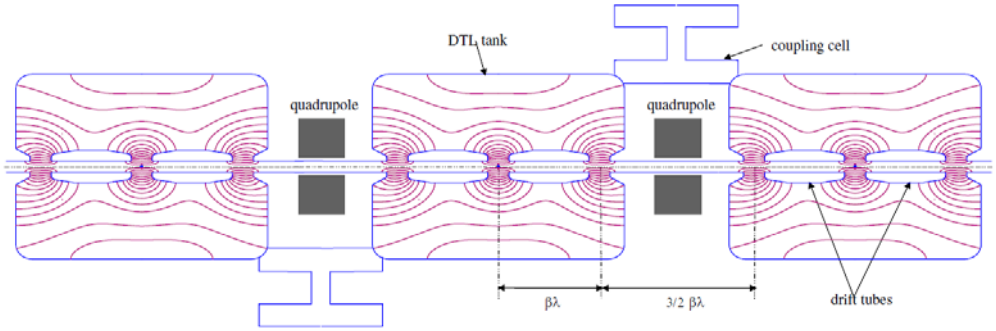

Figure 6.1 Scheme of a CCDTL module showing electric field lines[6].

Results of Path Manager simulations are reported below, using the DTL output beam as CCDTL input (see table X for twiss parameters). This beam has 89422 macro-particles and the input peak current is 62.6 mA.

Figures 6.2 and 6.3 show the RMS beam size and the RMS normalized emittances along the structure.

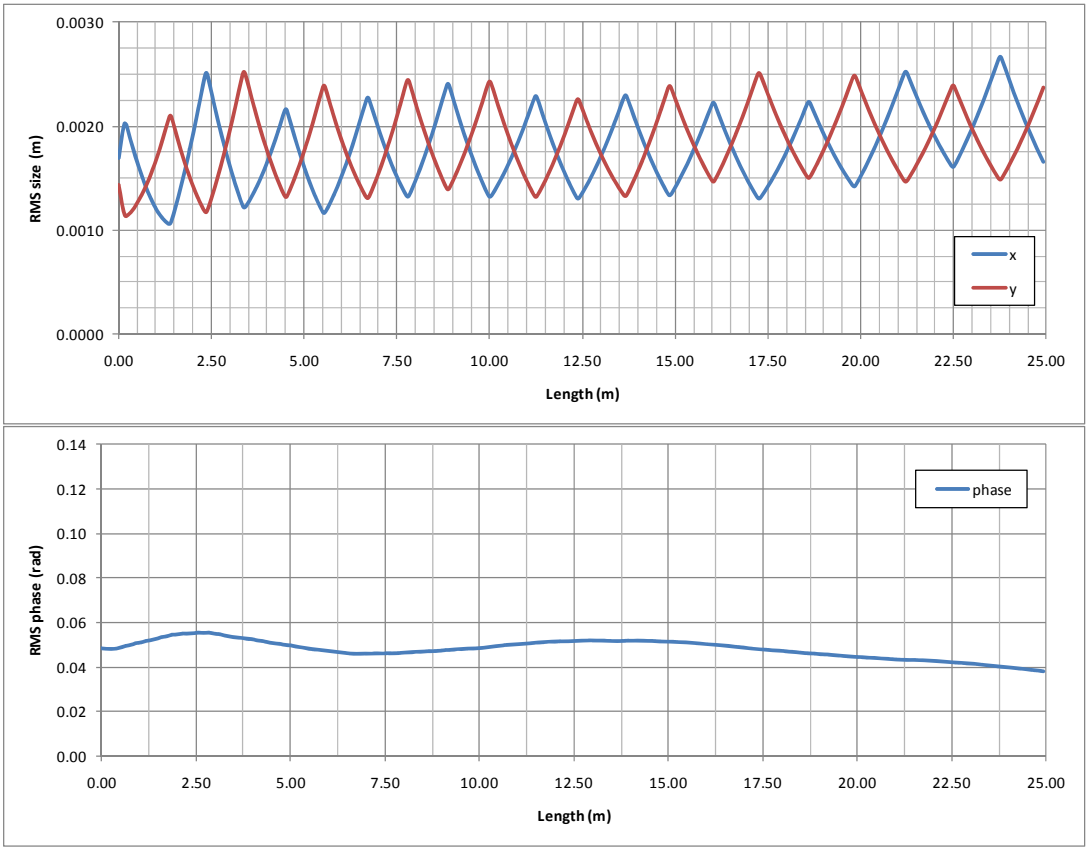

Figure 6.2 RMS beam size along the CCDTL.

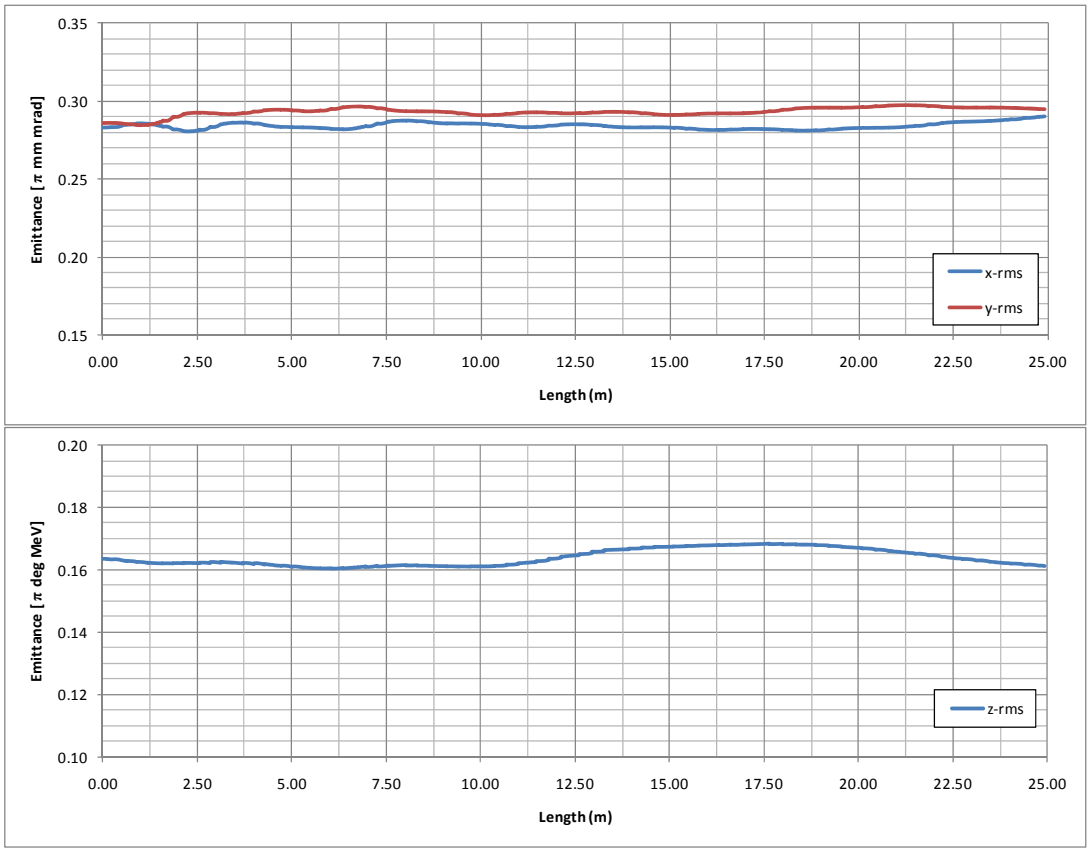

Figure 6.3 RMS normalized emittance in the CCDTL.

The transmission along the CCDTL is 100 %, and the output energy is 102.94 MeV.

The twiss parameters and the emittances at the end of CCDTL are summarized in table XII .The RMS and 90% emittance growth are reported in Table XIII.

	α	β	ε_{rms}	$\varepsilon_{90\%}$
x	1.98	4.53 mm/ π mrad	0.29 π mm mrad	1.22 π mm mrad
y	-3.64	9.17 mm/ π mrad	0.29 π mm mrad	1.23 π mm mrad
z	-0.42	29.39 deg/ π MeV	0.16 π deg MeV	0.68 π deg MeV

Table XII. CCDTL output beam parameters.

	ε_{rms}	$\varepsilon_{90\%}$
x	2.56 %	4.15 %
y	3.14 %	3.92 %
z	-1.91 %	0.72 %

Table XIII. RMS and 90% emittance growth in the CCDTL.

Figure 6.4 presents the CCDTL output beam shape, in the three phase spaces and in x-y.

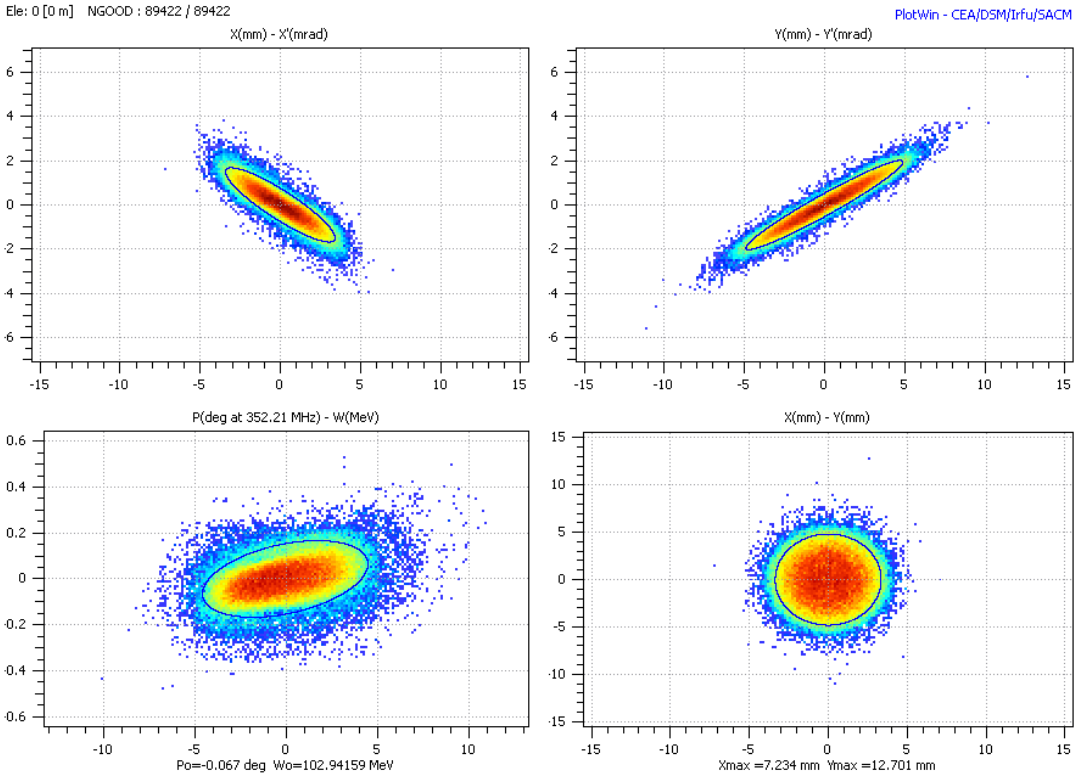

Figure 6.4 Beam phase space at the output of the CCDTL.

7. Beam dynamics in the PIMS

A Pi-mode accelerating structure, PIMS, consisting of 12 modules with 7 cells each, accelerates the beam from 102 MeV to 160 MeV. See figure 7.1. The total length is 22.85 meters.

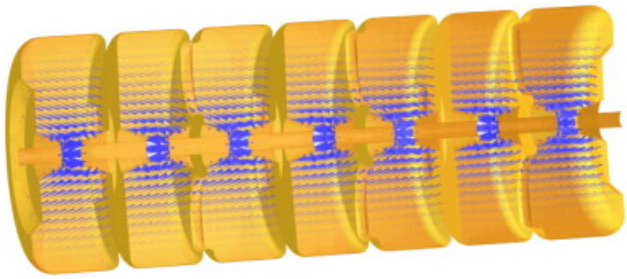

Figure 7.1 PIMS Module with Electric Field Lines.

Path Manager simulations results are reported below, using the CCDTL output as PIMS input beam (see table VIII for input twiss parameters). This beam has 89422 macro-particles and the input current is 62.6 mA.

The output average energy is 160.53 MeV.

Figures 7.2 and 7.3 show the RMS beam size and the RMS normalized emittances along the structure.

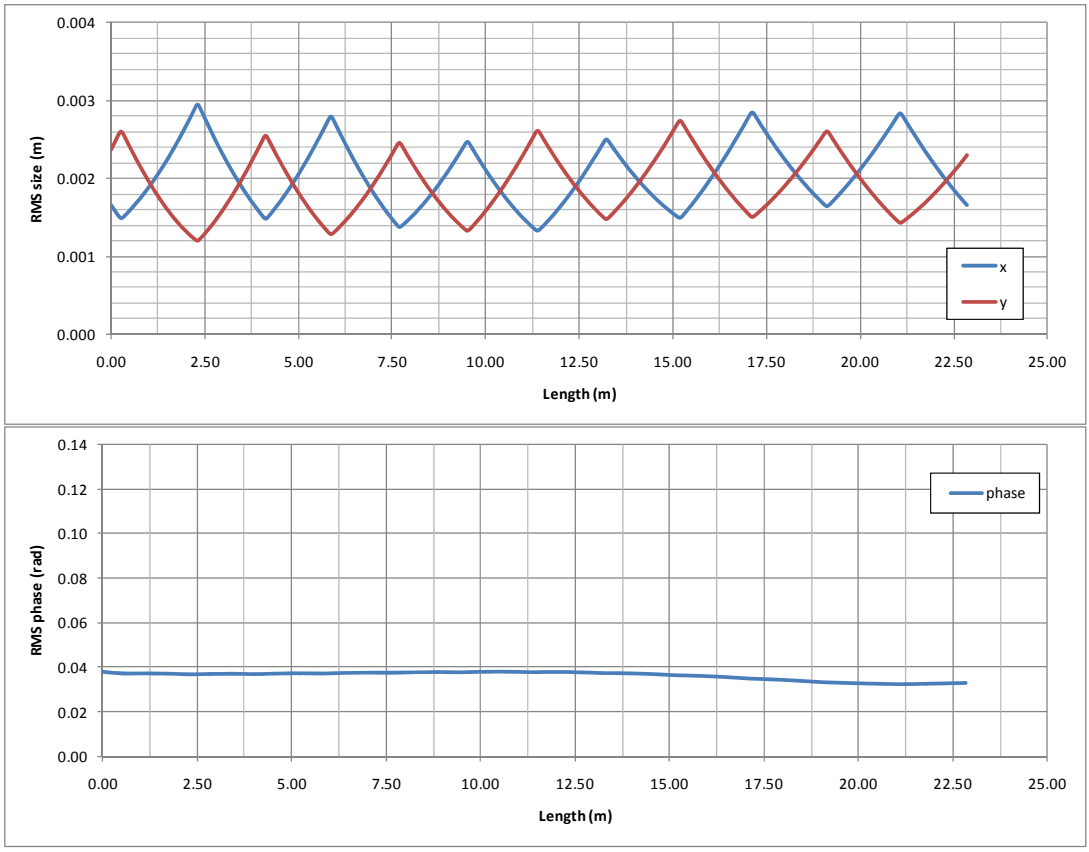

Figure 7.2 RMS beam size along the PIMS.

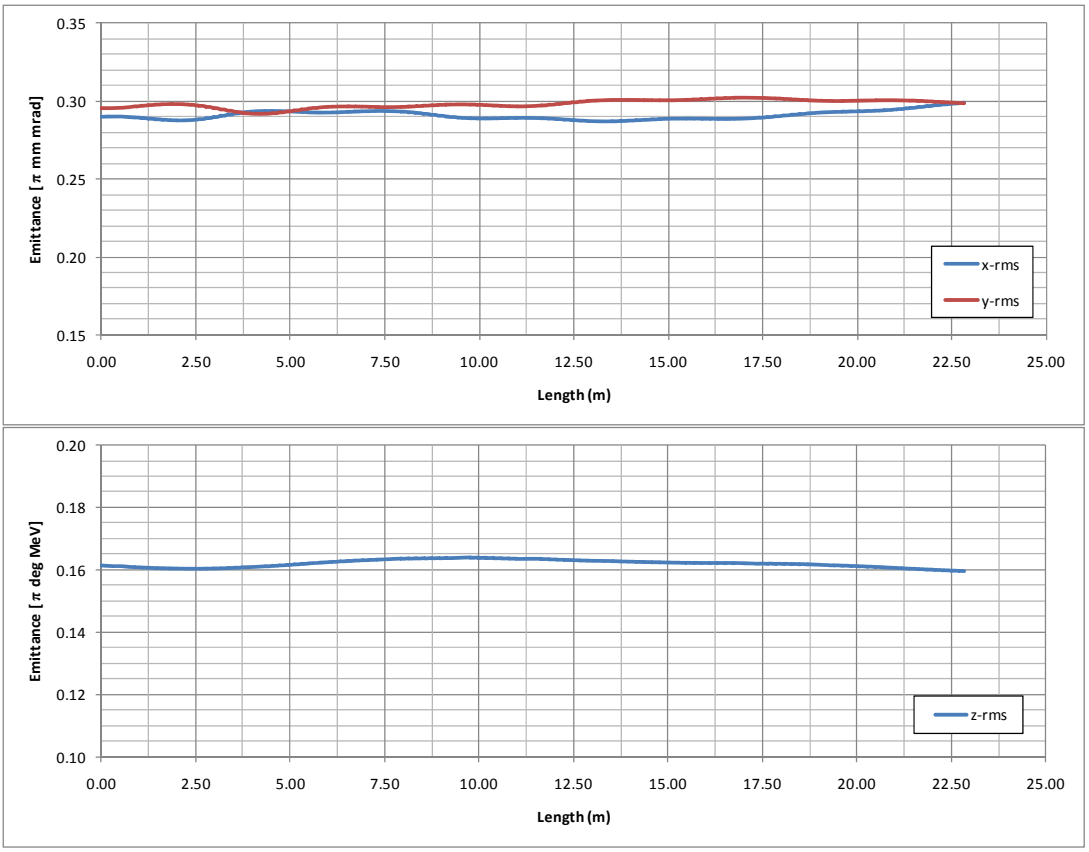

Figure 7.3 RMS normalized emittance along the PIMS.

The transmission along the PIMS is 100 %,

The twiss parameters and the emittances at the end of PIMS are summarized in the table below, and the RMS and 90% emittance growth are reported in Table XV.

	α	β	ε_{rms}	$\varepsilon_{90\%}$
x	1.77	5.56 mm/ π mrad	0.30 π mm mrad	1.26 π mm mrad
y	-2.95	10.79 mm/ π mrad	0.30 π mm mrad	1.25 π mm mrad
z	0.13	22.28 deg/ π MeV	0.16 π deg MeV	0.65 π deg MeV

Table XIV. PIMS output beam parameters.

	ε_{rms}	$\varepsilon_{90\%}$
x	3.27 %	3.04 %
y	1.08 %	1.29 %
z	-1.18 %	-4.21 %

Table XV. RMS and 90% emittance growth in the PIMS.

Figure 7.4 presents the PIMS output beam shape, in the three phase spaces and in x-y.

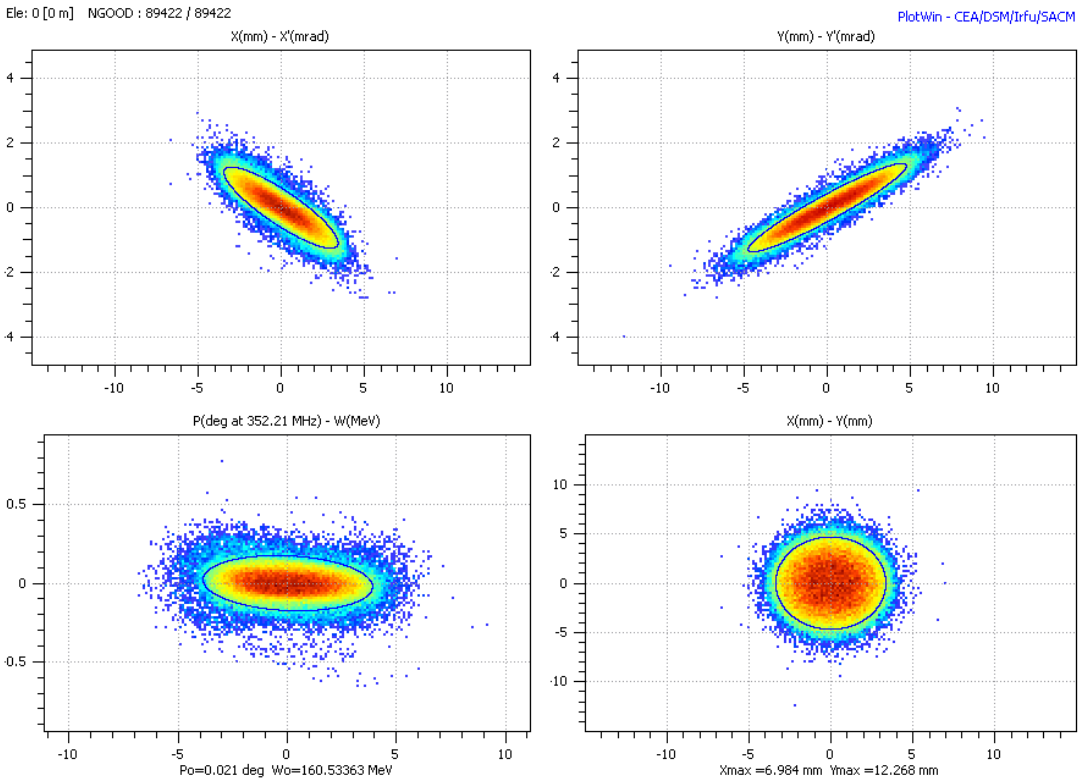

Figure 7.4 Beam phase space at the output of the PIMS. PlotWin.

8. End-to-end simulations (MEBT + DTL + CCDTL + PIMS)

In this section the results of the end-to-end simulation from 3 MeV to 160 MeV are presented, from the MEBT to the PIMS, in order to detect bottlenecks and mismatched points in the layout. The total length from the output of the RFQ up to the end of the PIMS is 70.73 m.

As in section 4, the output distribution of the RFQ was taken as MEBT input distribution, with 92841 macro-particles, and 65 mA peak current.

The figures of merit for the beam dynamics are: the losses, the rms emittance growth, the ratio of the rms beam size to the aperture and the sensitivity to errors.

The evolution of the rms emittance in the three planes is presented in Figures 8.1 , most of the emittance growth occurs in the chopper line (3.6 meters) as well as at the input of the DTL due to space charge effects. It then remains almost constant in the rest of the accelerator.

The output twiss parameters are identical to the ones obtained in the previous section as it was expected. See Table XIV and Figure 7.4.

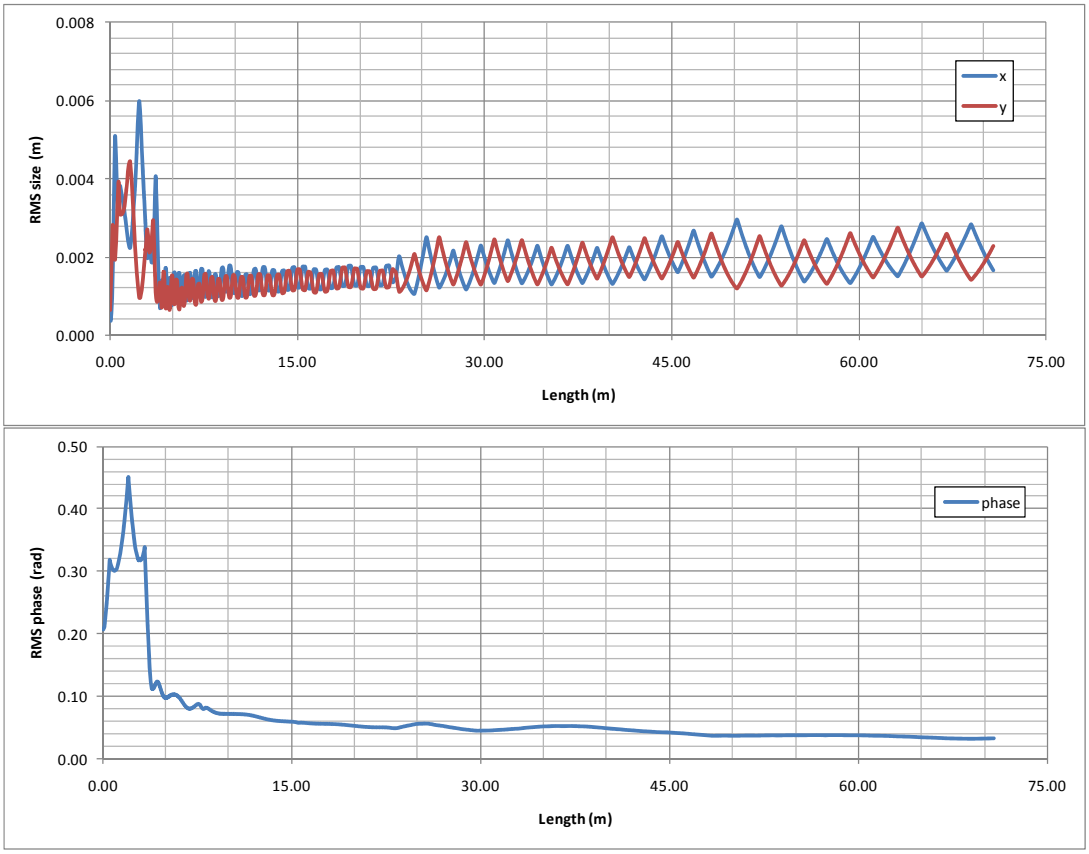

Figure 8.1 RMS beam size along Linac4.

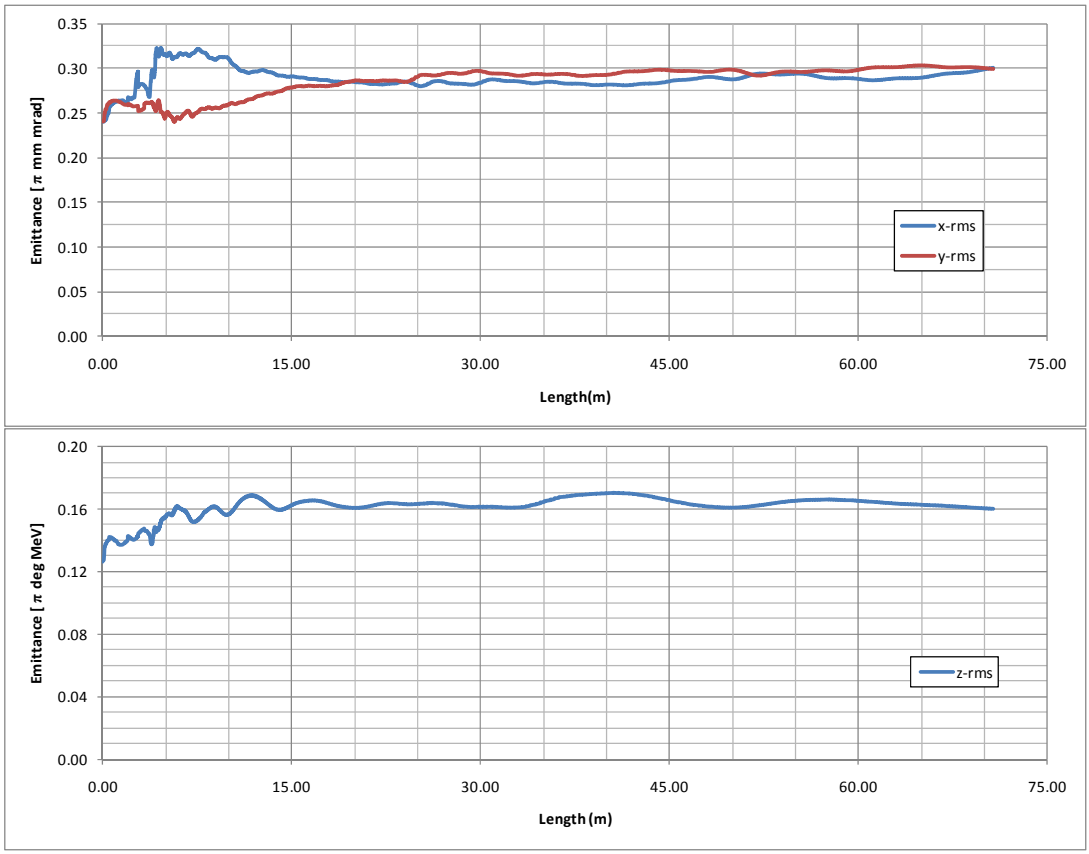

Figure 8.2 RMS normalized emittance along Linac4.

A quality factor of the solidity of the design is the ratio of the rms beam size to the radius of the vacuum chamber. In Figure 8.3 it is possible to see that the transverse bottleneck of LINAC4 is the chopper and the dump, where the aperture approaches the 2 rms beam size. Losses are localized in this area and the geometry of the chopper defines the minimum transverse acceptance of the whole Linac.

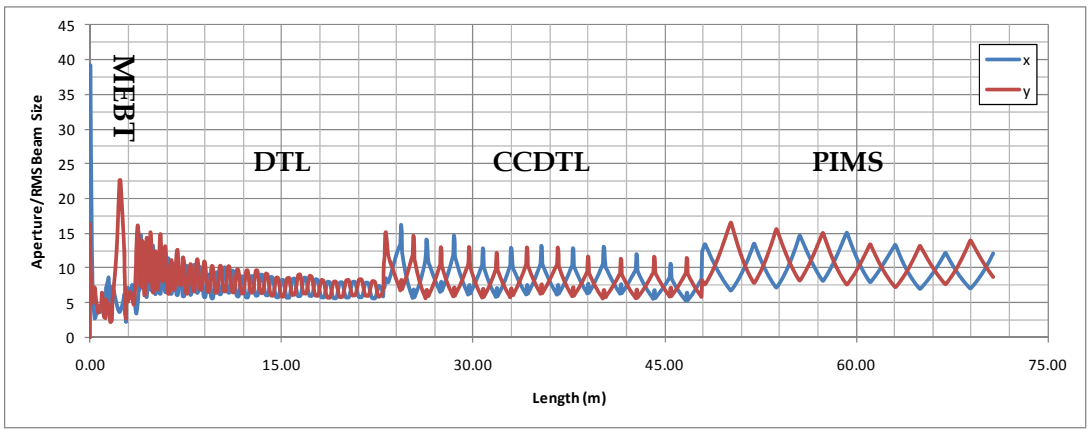

Figure 8.3 Aperture over the RMS size along Linac4.

The beam dynamics design and the afterwards end to end simulations and rematchings have been carried out taking care of fulfill the following constraints:

- A zero-current transverse phase advance below 90deg per period.
- Preserve a constant ratio of the longitudinal to transverse phase advance to avoid resonances and emittance exchange between transverse and longitudinal planes.
- Smooth variations of the transverse and longitudinal phase advance per meter.

Figure 8.4 shows the full current transverse phase advance per meter along the layout.

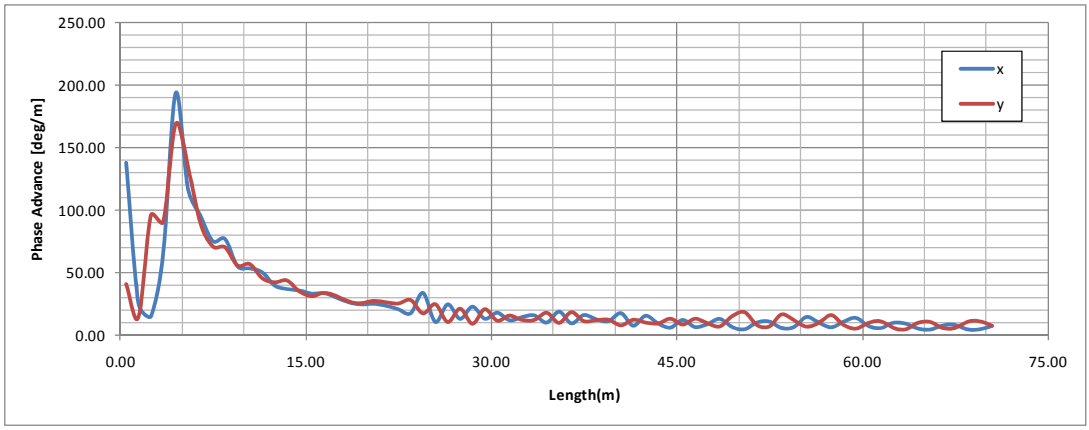

Figure 8.4 End to end beam phase advance along Linac4.

The energy gain in every structure is reported in figure 8.5.

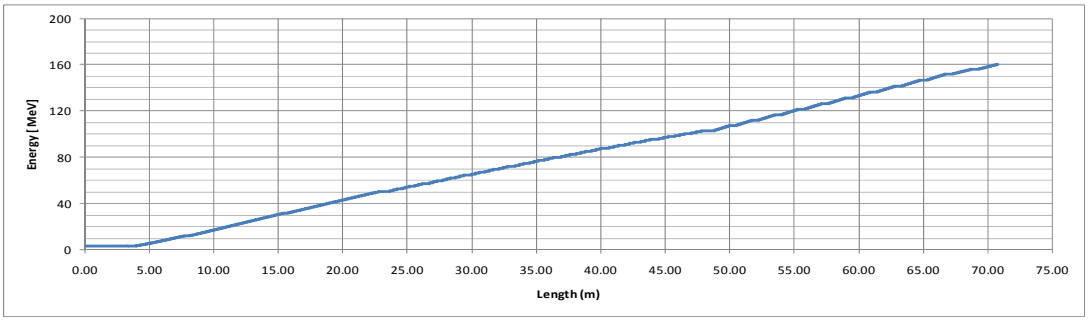

Figure 8.5 Average Kinetic Energy along the line.

Table XVI summarizes the emittance growth in the three planes for the whole Linac4.

	$\varepsilon_{x,rms}$	$\varepsilon_{y,rms}$	$\varepsilon_{z,rms}$	$\varepsilon_{x,90\%}$	$\varepsilon_{y,90\%}$	$\varepsilon_{z90\%}$
LEBT	8.16 %	8.37 %	-	18.56 %	18.86 %	-
RFQ	-9.96 %	-10.3 %	-	-3.33 %	-2.79 %	-
CHOPPER	22.50 %	8.91 %	8.61 %	21.59 %	8.54 %	11.80 %
DTL	-4.14 %	9.08 %	18.99 %	-6.07 %	6.18 %	16.04 %
CCDTL	2.56 %	3.14 %	-1.91%	4.15 %	3.92 %	0.72 %
PIMS	3.27 %	1.08 %	-1.18%	3.04 %	1.29 %	-4.21 %
Total	***22.39%***	***20.28%***	***24.51%***	***37.94%***	***36.00%***	***24.35%***

Table XVI. RMS and 90% emittance growth in Linac4.

9. Transfer Line and injection to the PSB

As part of the Linac4 project, a new branch of the transfer line was designed to join the present Linac2 transfer line at BHZ.20 (Figure 9.1). The layout of this part of the line is still being reviewed to obtain a better matching to the PSB [10]. The total length of the transfer line from the output of the linac to the PS Booster stripping foil is 177.35 meters

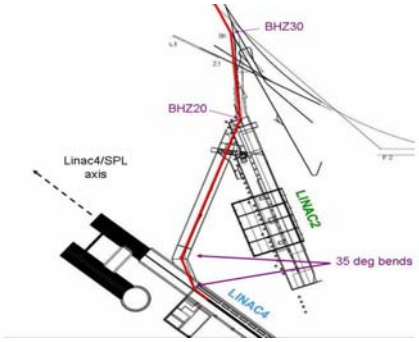

Figure 9.1 Transfer line layout (beam line shown in red).

Path Manager simulations results are reported below, using the PIMS output as TL input beam (see table XIV for input twiss parameters). This beam has 89422 macro-particles and the input current is 62.6 mA.

The output average energy is 160.82 MeV. Figures 9.2 and 9.3 show the RMS beam size and the RMS normalized emittances along the structure.

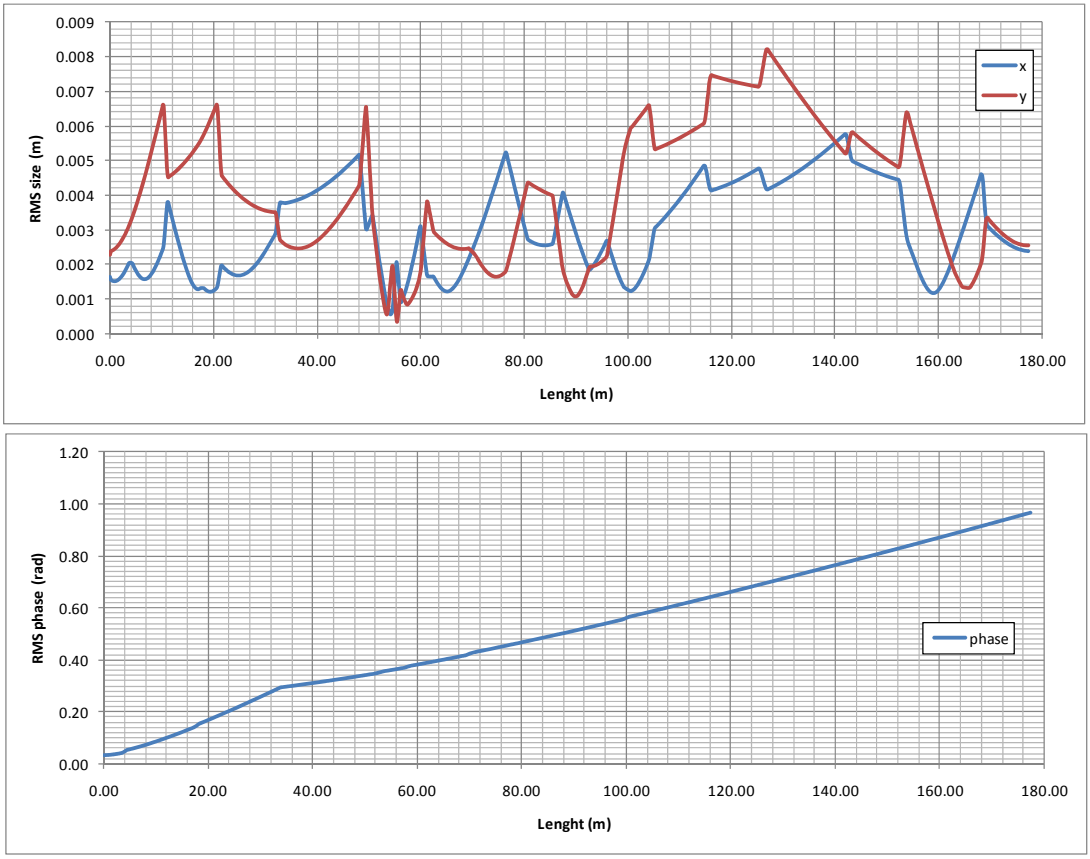

Figure 9.2 RMS beam size along the TL.

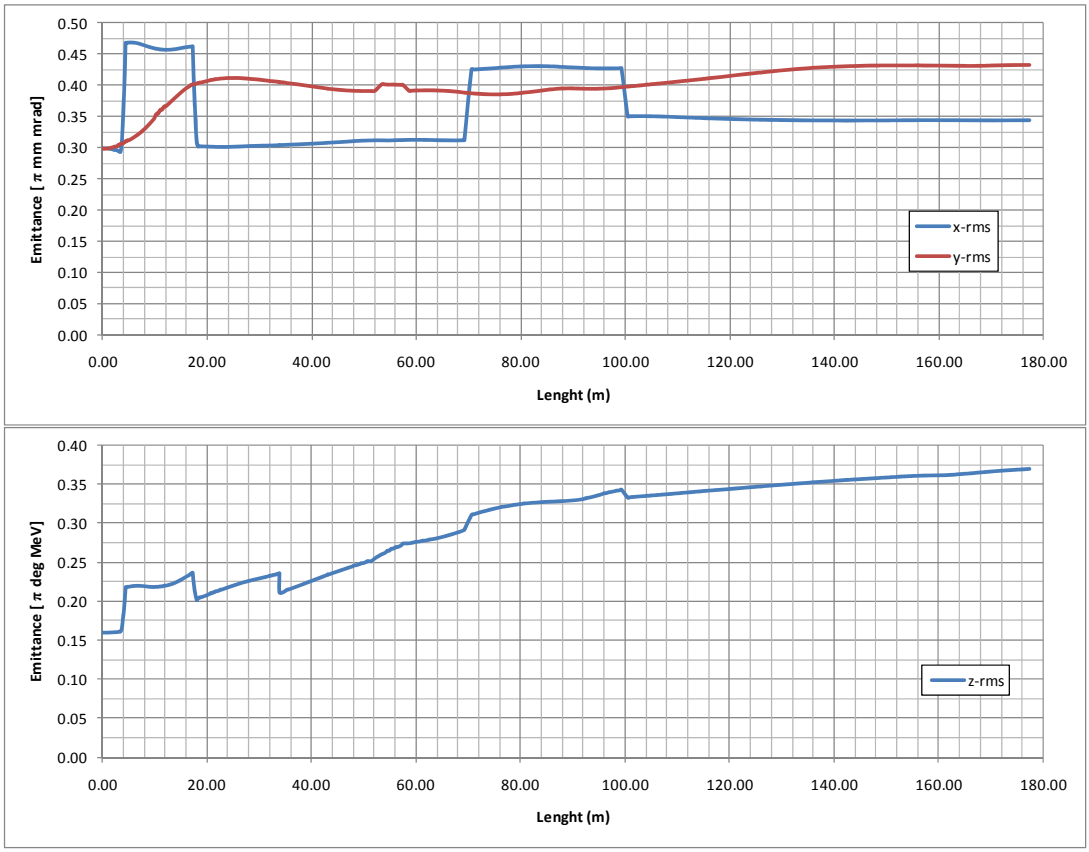

Figure 9.3 RMS normalized emittance along the TL.

The twiss parameters and the emittances at the end of TL are summarized in the table below, and the RMS and 90% emittance growth are reported in Table XV.

	α	β	ε_{rms}	$\varepsilon_{90\%}$
x	0.04	10.10 mm/ π mrad	0.34 π mm mrad	1.43 π mm mrad
y	-0.02	9.21 mm/ π mrad	0.43 π mm mrad	1.91 π mm mrad
z	23.89	8272.25 deg/ π MeV	0.37 π deg MeV	1.02 π deg MeV

Table XVII. PIMS output beam parameters.

	ε_{rms}	$\varepsilon_{90\%}$
x	15.13 %	13.78 %
y	44.62 %	52.36 %
z	130.97 %	57.08 %

Table XVIII. RMS and 90% emittance growth in the PIMS.

10. Beam dynamics Chopper ON

Until this chapter, the chopper was assumed to be OFF to let the beam being transmitted to the PSB. In this section the impact of switching ON the chopper is discussed.

As it was mentioned in section 4, the chopper gives the time structure to the beam avoiding losses at high energy being a key structure for the implementation of the longitudinal painting schemes at PSB injection. For this reason the chopping efficiency becomes an important parameter of Linac4.

PathManager simulations assuming 700 volts applied to the chopper plates were performed to study the fate of non-properly chopped particles, the losses along the line and the transmission to the booster. Field maps were used to model the chopper plates taking into account a field coverage factor of 0.76 (effective field).

The chopping efficiency is 99.93%, this means that s a few particles will not be stopped by the dump and will pass through it. In terms of peak current, 41μA (out of 62.6 mA when the chopper is off) will be transmitted into the DTL. Tracking this remaining beam along the linac, 23% is reported to be lost in the DTL, and around 77% will be accelerated and transmitted to the PSB. No losses are expected neither in the CCDTL nor in the PIMS. In the TL they are almost negligible [11], and in all cases the losses are well below the 1W/m limit for hands-on maintenance [12].

The transmission ratio to PS Booster is 0.06% of the chopper line input beam (65 mA).

Figure 10.1 illustrates the shape in x-y of the beam for both cases, chopper on and off.

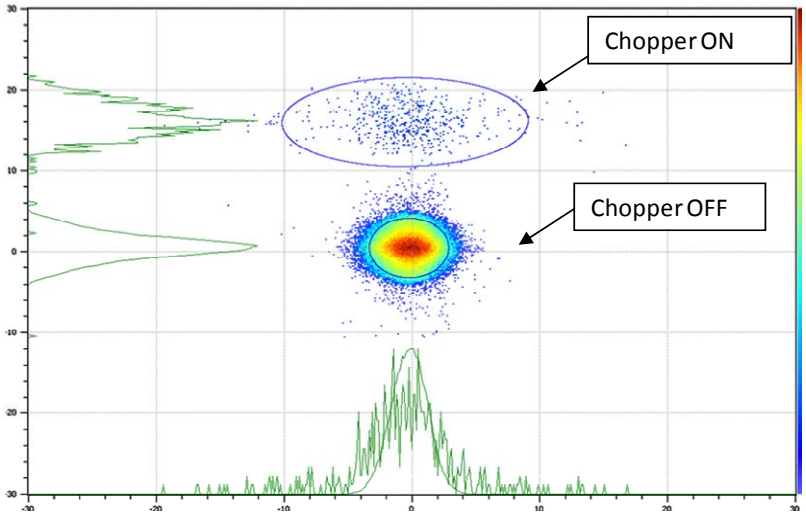

Figure 10.1 TL output beam (Nominal beam and deflected beam superimposed).

11. Machine hardware review

In this section a review of the hardware required for Linac4 is presented as well as a global view of the hardware settings which define the layout.

The quadrupole settings in the linac are shown in figure 11.1. The permanent quadrupoles are represented in red whereas the electromagnets quads are plotted in blue. A further description of the magnets parameters can be seen in Appendix B.

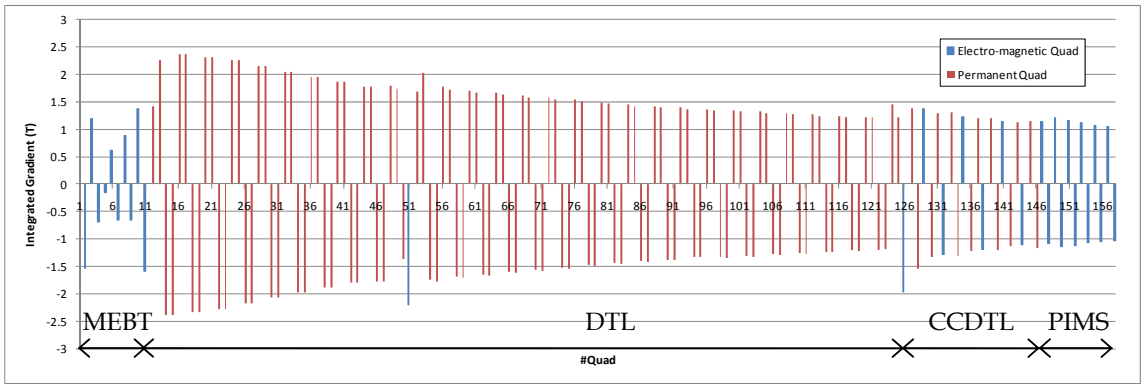

Figure 11.1 Quadrupoles settings.

The RF gaps/cavities along the layout are characterized by the voltage and the synchronous phase. Figure 11.2 represent these parameters.

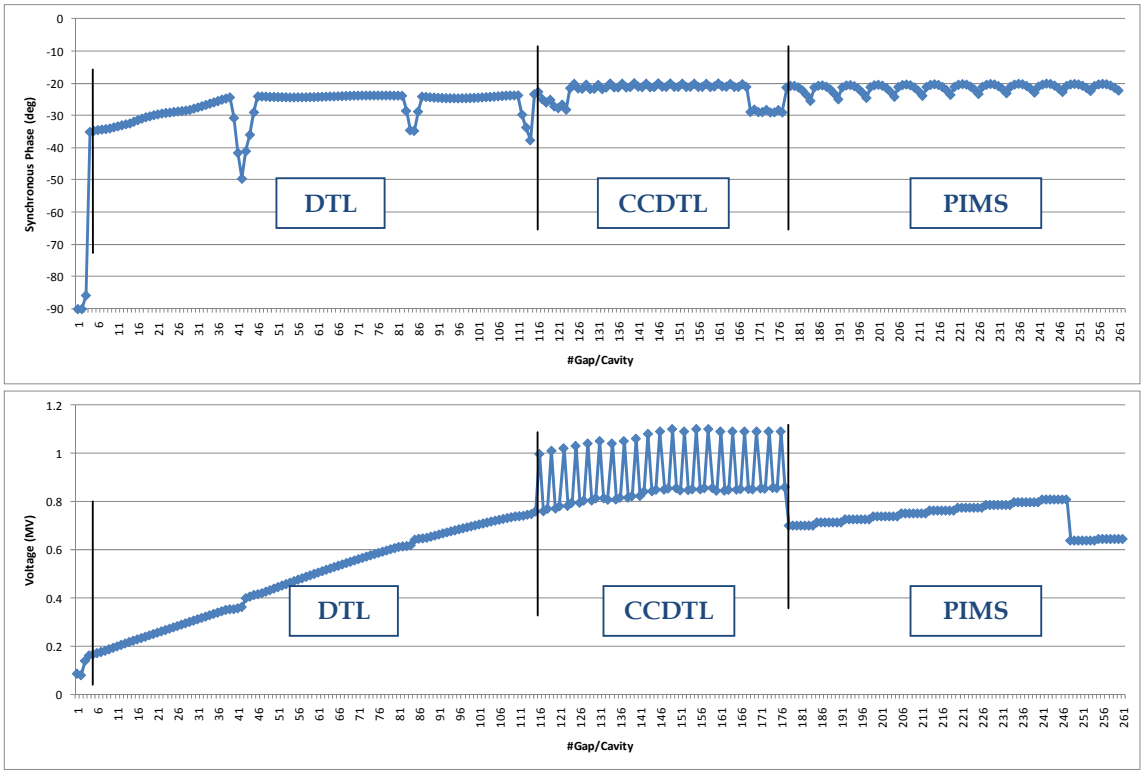

Figure 11.2 Cavities settings.

The following table summarizes the hardware included for each structure in the layout and the total number of elements included in Linac4.

Structure	#Solenoid	# PMQ	# EMQ	# Total Quads	# Buncher /Debuncher	#Bendings	# Steerers
LEBT	2	-	-	-	-	-	2
MEBT	-	-	11	11	3	-	-
DTL	-	114	1	115	-	-	2
CCDTL	-	14	7	21	-	-	4
PIMS	-	-	12	12	-	-	6
TL (New part)	-	-	16	16	1	5	13
Linac4	**2**	**118**	**47**	**175**	**4**	**5**	**27**

Table XVII. Linac4 Hardware review.

12. Conclusions

The new layout of Linac4 has been simulated from 45 keV to 160 MeV, and the performance will be compliant with the PSB requirements.

Most of the emittance growth occurs in the Chopper line, and it is level off downstream at the DTL output. Along the rest of the line the emittance remains almost constant; this proves that the different structures are well matched.

The transverse bottleneck of LINAC4 is the chopper line and in particular the dump which acts as rudimentary collimator. The particles which could be lost downstream are stopped at 3 MeV to avoid activation. In this area the aperture approaches the 2 rms beam size. Main losses are localized in the dump and the geometry of the chopper defines the minimum transverse acceptance of the whole LINAC.

13. References

[1] S. Lanzone, J.B. Lallement, A. Lombardi, E. Sargsyan, “End-to-end simulations of Linac4”. AB-Note-2006-033 ABP

[2] A.M. Lombardi, C. Rossi, M. Vretenar, “Design of an RFQ Accelerator optimized for Linac4 and SPL”. CERN-AB-2007-027- RF

[3] A. Perrin and J.F Amand, Travel v4.07, users manual,CERN (2003).

[4] R.Duperrier, N. Pichoff, D. Uriot, “CEA Saclay codes review”, ICCS Conference 2002, Amsterdam

[5] JB. Lallement, A. Lombardi, “Reducing the beam current in Linac4 in pulse to pulse mode”. CERN-BE-Note-2009-023

[6] F. Gerigk, M. Vretenar editors, “LINAC4 Technical Design Report”, CERN-AB-2006-084 ABP/RF

[7] P.-Y. Beauvais, “Recent evolutions in the design of the French high intensity proton injector (IPHI)”, Proc. 9th European Particle Accelerator Conf., Lucerne, Switzerland, 2004.

[8] K. R. Crandall et. al., ”RFQ Design Codes”, LA-UR-96-1836.

[9] J. Stovall, K. Crandall, E. Sargsyan, JB Lallement ,“Comparison of LINAC-4 designs” . CERN-BE-Note-2009-022

[10] L. Hein, C. Carli, A. Lombardi, “Update of the Linac4-PSB Transfer Line”. sLHC note (to be published)

[11] M. Garcia Tudela, JB. Lallement, A. Lombardi, “Chopper Line Studies”, CERN-sLHC-Project-Note-0012

[12] N.V Mokhov and W.Chou editors, “Beam Halo and scraping”, Proc. 7th ICFA mini-workshop on high intensity and high brightness hadron beams, Interlaken resort, Wisconsin, United States, 1999

Appendix A: Parameter List

Parameter	Value
General linac parameter	
Ion species	H-
Total length	70.73m
Output Energy	160.53 MeV
RF frequency	352.2 MHz
Repetition rate	1 Hz
Duty cycle	0.04%
Linac avg pulse current	40 mA
Average current	0.032 mA
Particles per pulse	1.0×10^{14}
Particles per bunch	1.14×10^{9}
Source and LEBT	
Source current	80 mA
Extraction Voltage	45 keV
LEBT length	1.82 m
Transverse output emittance	0.25 π.mm.mrad
RFQ	
Input Energy	45 keV
Output Energy	3 MeV
Peak current	70 mA
Average pulse current	70 mA
MEBT	
Input/Output Energy	3 MeV
RF Frequency	352.2 MHz
Peak current (I/O)	65/62.5 mA
Average pulse current (I/O)	65/40 mA
Total Length	3.9 m
Number chopper units	2
Chopper plate voltage	700 V
Effective chopper plate voltage	532 V
Chopper plate distance	20 mm
Length chopper plate	400 mm
DTL	
Input Energy	3MeV
Ouput Energy	50.28 MeV
RF Frequency	352.2 MHz
Peak current	62.5 mA
Average pulse current	40 mA
Total Length	19.08 m
CCDTL	
Input Energy	50.28 MeV
Ouput Energy	102.94 MeV
RF Frequency	352.2 MHz
Peak current	62.5 mA
Average pulse current	40 mA
Total Length	24.9 m
PIMS	
Input Energy	102.94 MeV
Ouput Energy	160.53 MeV

RF Frequency	352.2 MHz
Peak current	62.5 mA
Average pulse current	40 mA
Total Length	22.84 m

TL	
Input Energy	160.53 MeV
Ouput Energy	160.53 MeV
RF Frequency	352.2 MHz
Peak current	62.5 mA
Average pulse current	40 mA
Total Length	177.35 m
Number of bendings	5

Appendix B: Focusing elements parameters

Structure	Solenoid Name	Length (m)	Current (A)	Ap. radius (cm)	TYPE
LEBT	L4L.MLF.1120	0.190	628	28	II
	L4L.MLF.1220	0.190	557	28	II
Structure	Quad Name	Length (m)	Gradient (T/m)	Ap. radius (cm)	Integrated Gradient
MEBT	L4L.MQD.3110	0.056	30.0538	1.4	1.6830128
	L4L.MQF.3210	0.056	-27.4295	1.4	-1.536052
	L4L.MQD.3310	0.056	21.2108	1.4	1.1878048
	L4L.MQF.3410	0.056	-12.4477	1.4	-0.6970712
	L4L.MQF.3510	0.255	-0.599318	1	-0.15282609
	L4L.MQD.3610	0.255	2.43784	1	0.6216492
	L4L.MQF.3710	0.155	-4.27304	2.2	-0.6623212
	L4L.MQD.3810	0.082	10.8001	1.4	0.8856082
	L4L.MQF.3910	0.082	-7.99778	1.4	-0.65581796
	L4L.MQD.4010	0.056	24.5224	1.4	1.3732544
	L4L.MQF.4110	0.056	-28.3095	1.4	-1.585332
DTL	L4D.MQDP.0130	0.045	31.3752	1	1.411884
	L4D.MQDP.0131	0.045	50.3308	1	2.264886
	L4D.MQFP.0132	0.045	-53.0998	1	-2.389491
	L4D.MQFP.0133	0.045	-53.0998	1	-2.389491
	L4D.MQDP.0134	0.045	52.7564	1	2.374038
	L4D.MQDP.0135	0.045	52.7564	1	2.374038
	L4D.MQFP.0136	0.045	-51.8382	1	-2.332719
	L4D.MQFP.0137	0.045	-51.8382	1	-2.332719
	L4D.MQDP.0138	0.045	51.5172	1	2.318274
	L4D.MQDP.0139	0.045	51.5172	1	2.318274
	L4D.MQFP.0140	0.045	-50.6265	1	-2.2781925
	L4D.MQFP.0141	0.045	-50.6265	1	-2.2781925
	L4D.MQDP.0142	0.045	50.0457	1	2.2520565
	L4D.MQDP.0143	0.045	50.0457	1	2.2520565
	L4D.MQFP.0144	0.045	-48.3483	1	-2.1756735
	L4D.MQFP.0145	0.045	-48.3483	1	-2.1756735
	L4D.MQDP.0146	0.045	47.7604	1	2.149218
	L4D.MQDP.0147	0.045	47.7604	1	2.149218
	L4D.MQFP.0148	0.045	-46.0324	1	-2.071458
	L4D.MQFP.0149	0.045	-46.0324	1	-2.071458
	L4D.MQDP.0150	0.045	45.4924	1	2.047158
	L4D.MQDP.0151	0.045	45.4924	1	2.047158
	L4D.MQFP.0152	0.045	-43.8998	1	-1.975491
	L4D.MQFP.0153	0.045	-43.8998	1	-1.975491
	L4D.MQDP.0154	0.045	43.3707	1	1.9516815
	L4D.MQDP.0155	0.045	43.3707	1	1.9516815
	L4D.MQFP.0156	0.045	-41.7978	1	-1.880901
	L4D.MQFP.0157	0.045	-41.7978	1	-1.880901
	L4D.MQDP.0158	0.045	41.2961	1	1.8583245
	L4D.MQDP.0159	0.045	41.2961	1	1.8583245
	L4D.MQFP.0160	0.045	-39.7977	1	-1.7908965
	L4D.MQFP.0161	0.045	-39.7977	1	-1.7908965
	L4D.MQDP.0162	0.045	39.3649	1	1.7714205
	L4D.MQDP.0163	0.045	39.3649	1	1.7714205
	L4D.MQFP.0164	0.045	-39.4307	1	-1.7743815
	L4D.MQFP.0165	0.045	-39.4307	1	-1.7743815
	L4D.MQDP.0166	0.045	39.8714	1	1.794213
	L4D.MQDP.0167	0.045	38.6397	1	1.7387865
	L4D.MQFP.0168	0.045	-30.1966	1	-1.358847
	L4D.MQD.0210	0.105	-20.9373	1	-2.1984165
	L4D.MQDP.0230	0.045	37.363	1	1.681335
	L4D.MQDP.0231	0.08	25.3892	1	2.031136
	L4D.MQFP.0232	0.08	-21.8698	1	-1.749584
	L4D.MQFP.0233	0.08	-22.184	1	-1.77472
	L4D.MQDP.0234	0.08	22.1196	1	1.769568
	L4D.MQDP.0235	0.08	21.4849	1	1.718792
	L4D.MQFP.0236	0.08	-21.1266	1	-1.690128
	L4D.MQFP.0237	0.08	-21.4237	1	-1.713896
	L4D.MQDP.0238	0.08	21.4094	1	1.712752
	L4D.MQDP.0239	0.08	20.862	1	1.66896
	L4D.MQFP.0240	0.08	-20.5724	1	-1.645792
	L4D.MQFP.0241	0.08	-20.8473	1	-1.667784
	L4D.MQDP.0242	0.08	20.8345	1	1.66676
	L4D.MQDP.0243	0.08	20.3156	1	1.625248
	L4D.MQFP.0244	0.08	-20.0362	1	-1.602896
	L4D.MQFP.0245	0.08	-20.2909	1	-1.623272
	L4D.MQDP.0246	0.08	20.2791	1	1.622328
	L4D.MQDP.0247	0.08	19.7858	1	1.582864
	L4D.MQFP.0248	0.08	-19.5151	1	-1.561208
	L4D.MQFP.0249	0.08	-19.7512	1	-1.580096
	L4D.MQDP.0250	0.08	19.7407	1	1.579256
	L4D.MQDP.0251	0.08	19.2712	1	1.541696
	L4D.MQFP.0252	0.08	-19.0089	1	-1.520712
	L4D.MQDP.0253	0.08	-19.2281	1	-1.538248
	L4D.MQDP.0254	0.08	19.2185	1	1.53748
	L4D.MQDP.0255	0.08	18.7702	1	1.501616
	L4D.MQFP.0256	0.08	-18.5147	1	-1.481176
	L4D.MQFP.0257	0.08	-18.7184	1	-1.497472
	L4D.MQDP.0258	0.08	18.7099	1	1.496792
	L4D.MQDP.0259	0.08	18.2803	1	1.462424
	L4D.MQFP.0260	0.08	-18.0304	1	-1.442432
	L4D.MQFP.0261	0.08	-18.2199	1	-1.457592

DTL	L4D.MQDP.0262	0.08	18.2121	1	1.456968
	L4D.MQDP.0263	0.08	17.7998	1	1.423984
	L4D.MQFP.0264	0.08	-17.5548	1	-1.404384
	L4D.MQFP.0265	0.08	-17.7313	1	-1.418504
	L4D.MQDP.0266	0.08	17.7243	1	1.417944
	L4D.MQDP.0267	0.08	17.4009	1	1.392072
	L4D.MQFP.0268	0.08	-17.2211	1	-1.377688
	L4D.MQFP.0269	0.08	-17.3869	1	-1.390952
	L4D.MQDP.0270	0.08	17.3954	1	1.391632
	L4D.MQDP.0271	0.08	17.0996	1	1.367968
	L4D.MQFP.0272	0.045	-29.7359	1	-1.3381155
	L4D.MQFP.0330	0.045	-29.7359	1	-1.3381155
	L4D.MQDP.0331	0.08	16.9285	1	1.35428
	L4D.MQDP.0332	0.08	16.7286	1	1.338288
	L4D.MQFP.0333	0.08	-16.6809	1	-1.334472
	L4D.MQFP.0334	0.08	-16.832	1	-1.34656
	L4D.MQDP.0335	0.08	16.8268	1	1.346144
	L4D.MQDP.0336	0.08	16.5349	1	1.322792
	L4D.MQFP.0337	0.08	-16.3797	1	-1.310376
	L4D.MQFP.0338	0.08	-16.5222	1	-1.321776
	L4D.MQDP.0339	0.08	16.5171	1	1.321368
	L4D.MQDP.0340	0.08	16.2166	1	1.297328
	L4D.MQFP.0341	0.08	-16.0447	1	-1.283576
	L4D.MQFP.0342	0.08	-16.1787	1	-1.294296
	L4D.MQDP.0343	0.08	16.174	1	1.29392
	L4D.MQDP.0344	0.08	15.8834	1	1.270672
	L4D.MQFP.0345	0.08	-15.7141	1	-1.257128
	L4D.MQFP.0346	0.08	-15.8403	1	-1.267224
	L4D.MQDP.0347	0.08	15.8359	1	1.266872
	L4D.MQDP.0348	0.08	15.5542	1	1.244336
	L4D.MQFP.0349	0.08	-15.3869	1	-1.230952
	L4D.MQFP.0350	0.08	-15.5058	1	-1.240464
	L4D.MQDP.0351	0.08	15.5018	1	1.240144
	L4D.MQDP.0352	0.08	15.2277	1	1.218216
	L4D.MQFP.0353	0.08	-15.0609	1	-1.204872
	L4D.MQFP.0354	0.08	-15.1731	1	-1.213848
	L4D.MQDP.0355	0.08	15.1699	1	1.213592
	L4D.MQDP.0356	0.08	15.2808	1	1.222464
	L4D.MQFP.0357	0.08	-15	1	-1.2
	L4D.MQFP.0358	0.08	-14.9284	1	-1.194272
	L4D.MQDP.0359	0.08	18.2592	1	1.460736
	L4D.MQDP.0360	0.045	27.208	1	1.22436
CCDTL	L4C.MQF.0110	0.105	-18.8053	1.7	-1.9745565
	L4C.MQDP.0145	0.1	13.7734	1.7	1.37734
	L4C.MQFP.0165	0.1	-15.456	1.7	-1.5456
	L4C.MQD.0210	0.105	13.12	1.7	1.3776
	L4C.MQFP.0245	0.1	-13.3359	1.7	-1.33359
	L4C.MQDP.0265	0.1	13.0003	1.7	1.30003
	L4C.MQF.0310	0.105	-12.3058	1.7	-1.292109
	L4C.MQDP.0345	0.1	13.0331	1.7	1.30331
	L4C.MQFP.0365	0.1	-13.0295	1.7	-1.30295
	L4C.MQD.0410	0.105	11.6703	1.7	1.2253815
	L4C.MQFP.0445	0.1	-12.2894	1.7	-1.22894
	L4C.MQDP.0465	0.1	12.0504	1.7	1.20504
	L4C.MQF.0510	0.105	-11.4243	1.7	-1.1995515
	L4C.MQDP.0545	0.1	12.0753	1.7	1.20753
	L4C.MQFP.0565	0.1	-12.0726	1.7	-1.20726
	L4C.MQD.0610	0.105	10.7998	1.7	1.133979
	L4C.MQFP.0645	0.1	-11.3607	1.7	-1.13607
	L4C.MQDP.0665	0.1	11.3688	1.7	1.13688
	L4C.MQF.0710	0.105	-10.5934	1.7	-1.112307
	L4C.MQDP.0745	0.1	11.4581	1.7	1.14581
	L4C.MQFP.0765	0.1	-11.6865	1.7	-1.16865
PIMS	L4P.MQD.0110	0.105	10.8032	2	1.134336
	L4P.MQF.0210	0.105	-10.3165	2	-1.0832325
	L4P.MQD.0310	0.105	11.477	2	1.205085
	L4P.MQF.0410	0.105	-10.9454	2	-1.149267
	L4P.MQD.0510	0.105	10.9357	2	1.1482485
	L4P.MQF.0610	0.105	-10.6709	2	-1.1204445
	L4P.MQD.0710	0.105	10.6622	2	1.119531
	L4P.MQF.0810	0.105	-10.2097	2	-1.0720185
	L4P.MQD.0910	0.105	10.2038	2	1.071399
	L4P.MQF.1010	0.105	-10.0475	2	-1.0549875
	L4P.MQD.1110	0.105	10.0296	2	1.053108
	L4P.MQF.1210	0.105	-9.9	2	-1.0395